

“Structure of Complement C6 suggests a mechanism for initiation and unidirectional, sequential assembly of the Membrane Attack Complex (MAC)”

Alexander E. Aleshin, Ingrid U. Schraufstatter, Boguslaw Stec, Laurie A. Bankston, Robert C. Liddington & Richard G. DiScipio

SUPPLEMENTAL FIGURES 1-10

Supplemental Fig. 1. Stereo views of C6 and selected Electron Density.

Supplemental Fig. 2. Multiple sequence alignment of MAC components C6-C9.

Supplemental Fig. 3. Comparison of TS modules from C6 and thrombospondin-1.

Supplemental Fig. 4. Stereo and surface presentations of the CCP module of C6.

Supplemental Fig. 5. Ribbon and surface presentations of FIM modules from C6 and C7.

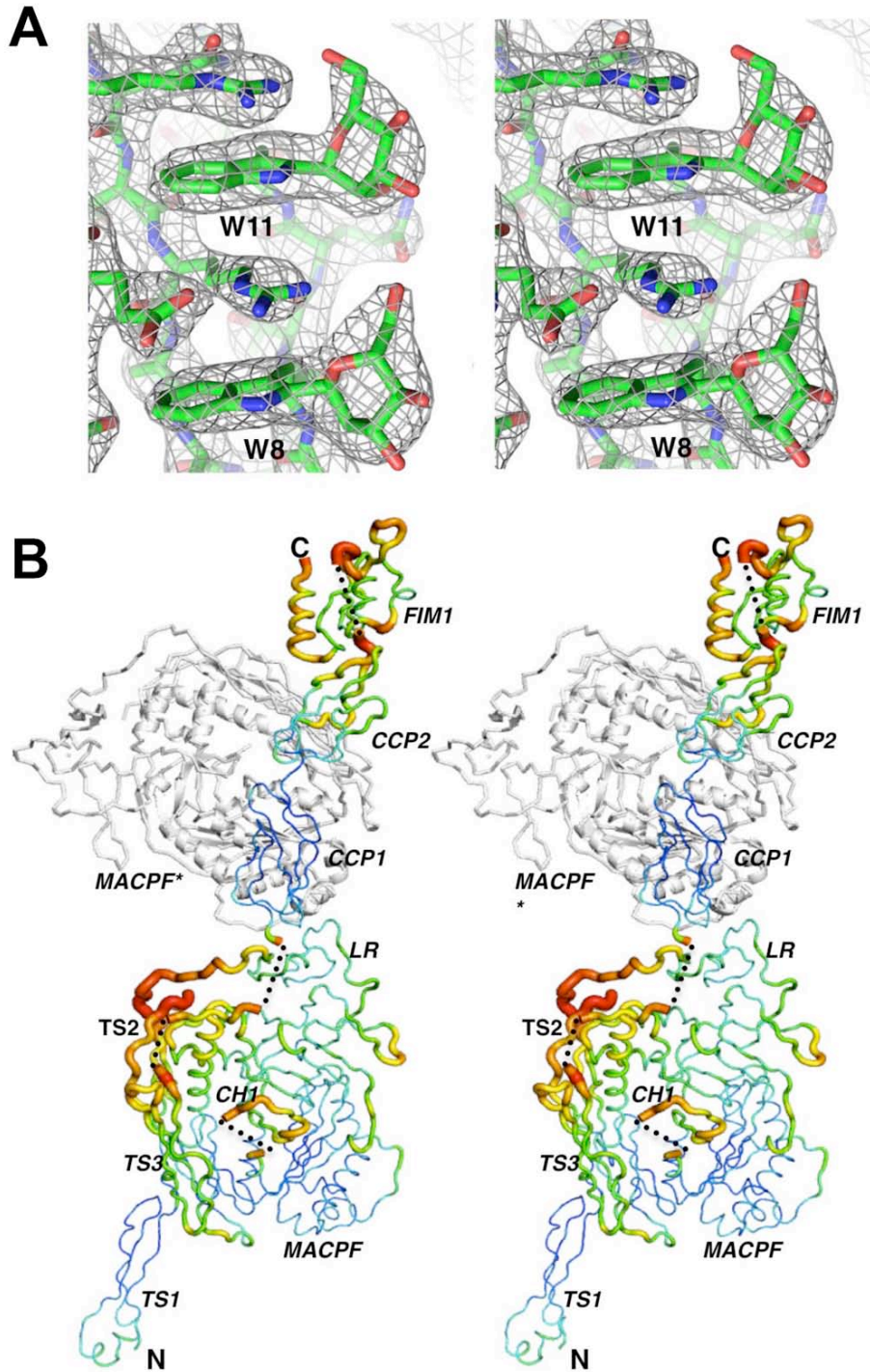
Supplemental Fig. 6. Modeling the position of CCP/FIMs in native C6.

Supplemental Fig. 7. Stereo views of superposed MACPFs in different reference frames and overlay with perforin.

Supplemental Fig. 8. Complementary charges on putative interacting surfaces of MAC components.

Supplemental Fig. 9. Sequence alignments of CH1 and CH2 (putative membrane-inserting elements) from vertebrate orthologs of C6 and C7.

Supplemental Fig. 10. Atomic model of the poly-C9 pore containing 18 subunits



Supplemental Fig. 1. Stereo views of C6 and selected Electron Density. *A*, Fragment of the C6 model fitted into the 2Fo-Fc electron density map, drawn at the 2.0- σ level. The tryptophans are glycosylated at C1 atom with α -mannose. *B*, The C6 molecule is shown as a Ca tube with the thickness and the color indicating the B-factors of Ca atoms (dark blue $\sim 60 \text{ \AA}^2$ and red $\sim 200 \text{ \AA}^2$). MACPF of a crystallographically related molecule (marked with *) is also shown as a gray ribbon. It may mimic C5b in the C5b-C6 complex, in separating the CCP modules and FIMs from the body of the MACPF.

TS1
 C6 1 CFC^DDHYAWTQWTS^CSKT^CNS^GTQSRHRQIVVDKYYQENF^CEQI^CSKQETRE^CNWQRCPIN 60
 C7 1 SSPVN 5
 C8 β 1 SVDVTLMPID 10
 C8 α 1 AATPAAVT 8
 C9 1 QYTTSYDPEL^TTESS^GSASHID 21

TS2
 C6 61 CLL^GD^FG^PW^SD^CD^PCIE^KQ^SK^VR^SV^LR^PS^QF^GG^QP^CTAP^LV^AF^QP^CI^PS^KL^CKIE^EAD^CK 120
 C7 6 CQWDFYAPWSE^CNG^CT^KT^QT^RR^RS^VA^VY^GQ^YG^GQ^PCV^GNA^FET^QS^CE^PT^RGCPT^EE^GC^G 64
 C8 β 11 CELSSWSSW^TTC^DPC^QK^KR^YAY^LL^QPS^QF^HG^EPC^NF^SDK^EV^EDC^VT^NRPCGS^QV^RC 68
 C8 α 9 CQLSNWSEW^TDC^FPC^QD^KK^YR^HR^SLL^QPN^KF^GGT^ICS^GD^IWD^QASC^SST^TCVR^QA^QC^G 67
 C9 22 CRMSPWSEW^SQC^DP^CL^RQM^FRS^RSE^IV^FG^QF^NG^KR^CTDA^VG^DRR^QCV^PT^EPC^EDA^EDD^CG 81

LR * * * * ** MACPF
 C6 121 NK^FRC-D^SG^RC^IA^RK^LE^CN^GE^ND^CG-D^NS^DE^RD^CG^RT^KA^VC^TR- - -K^YN^PI^PS^VQ^LM^GN^G 175
 C7 65 ER^FRC-F^SG^QC^IS^KS^LV^CN^GD^SD^CD^ED^SA^DE^DR^CD^ES^ER^RP^SC^DI^DK- -P^PP^NI^EL^TG^NG 121
 C8 β 69 E^GF^VC^AQ^TG^RC^VN^RR^LL^CN^GD^ND^CG-D^QS^DE^AN^CR^RI^YK^KQ^HE^MD^QY^WG^I-G^S- -L^AS^G 124
 C8 α 68 Q^DF^QC^KE^TG^RC^LK^RH^LV^CN^GD^QD^CL-D^GS^DE^DD^DC^ED^V-R^AI^DE^DC^SQ^YE^PI^PG^SQ^KA^LG 125
 C9 82 N^DF^QC-S^TG^RC^IK^MR^LR^CN^GD^ND^CG-D^FS^DE^DD^DC^ES^EP^RP^PC^RD^R-V^VE^ES^EL^AR^TA^GY^G 138

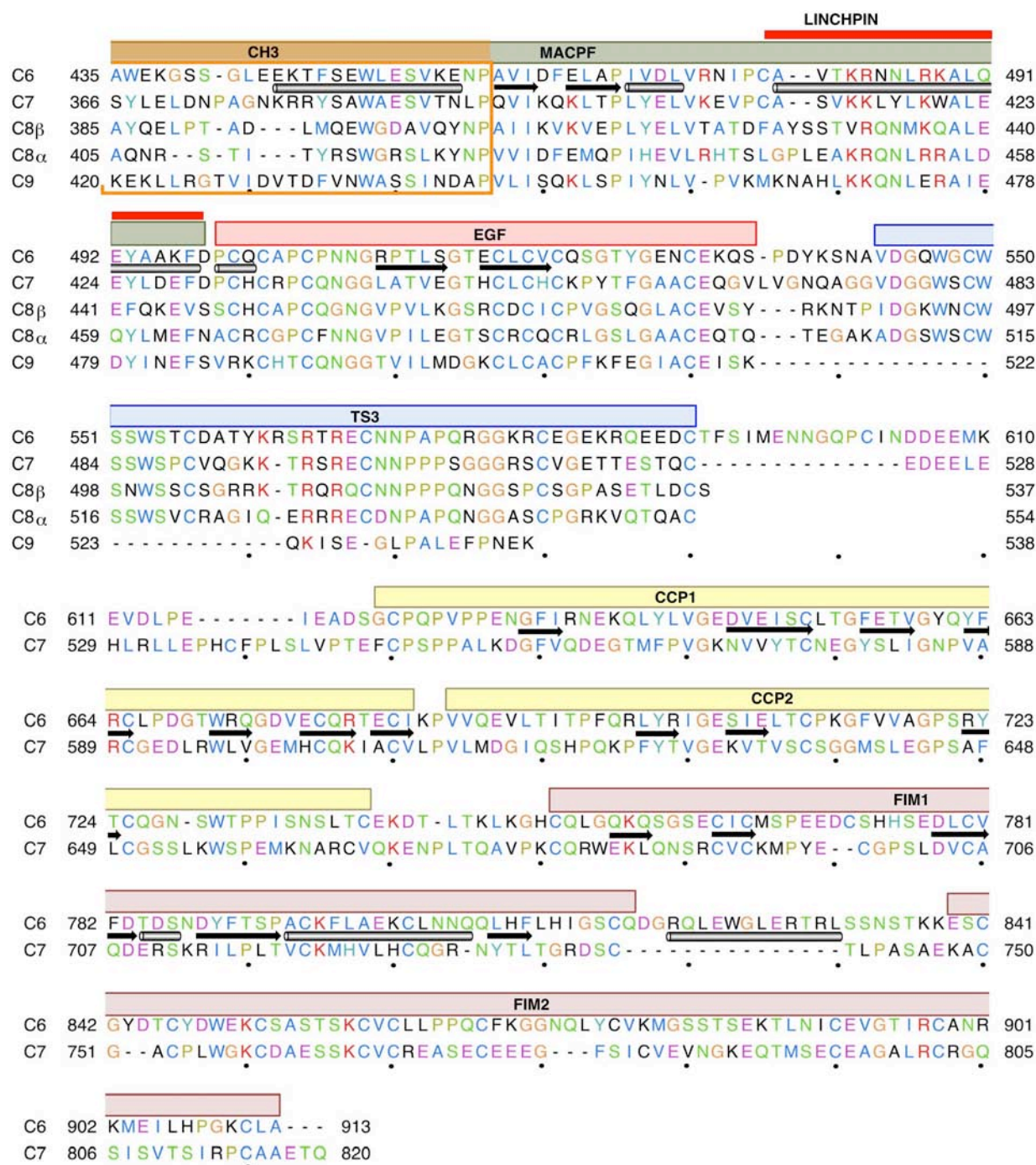
MACPF
 C6 176 F^HF^LA^GE^PR^GE^VL^DN^SF^TG^GI^CK^TV^KS^RT^S- - -N^PY^RV^PA^NL^EN^V 218
 C7 122 Y^NE^LT^GQ^FR^NR^VI^NT^KS^FG^GQ^CR^KV^FS^GD^GK- - -D^FY^RL^SG^NV^LS^Y 164
 C8 β 125 I^NL^FT^NS^FE^GP^VL^DH^RY^YA^GG^CS^PH^YI^LN^TR- - -F^RK^PY^NV^ES^Y 165
 C8 α 126 Y^NI^LT^QE^DA^QS^VY^DA^SY^YG^GQ^CE^TV^YN^GE^WR^EL^RY^DS^TC^ER^LY^YG^DD^EK^YF^RK^PY^NF^LK^Y 185
 C9 139 I^NI^LG^MD^PL^ST^PF^DN^EF^YN^GL^CN^RD^RD^GN^TL- - -T^YY^RR^PW^NV^AS^L 181

CH1
 C6 219 G^FE^VQ^TA^ED^DL^KT^DF^YK^DL^TS^LG^HN^EN^QQ^GS^FS^SQ^GS^SF^SV^P- - - 264
 C7 165 T^FQ^VK-I^NN^DF^NY^EF^YN^ST^WS^YV^KH^TS^TE^HT^SS^SR^KR^SF- - - 203
 C8 β 166 T^PQ^T-G^KY^EF^IL^KE^YE^SY^SD^FE^RN^VT^EK^MA^SK^SG^FS^FF^GF^KI^P- - - 207
 C8 α 186 H^FE^AL-A^DT^GI^SS^EF^YD^NA^ND^LL^SK^VK^KD^KS^DS^FG^VT^IG^IG^PA^G- - - 228
 C9 182 I^YE^TK-G^EK^NF^RT^EH^YE^QI^EA^FK^SI^IQ^EK^TS^NF^NA^AI^SL^KF^TP^TE^TN^KA^EQ^CC^EE^TA^SS 240

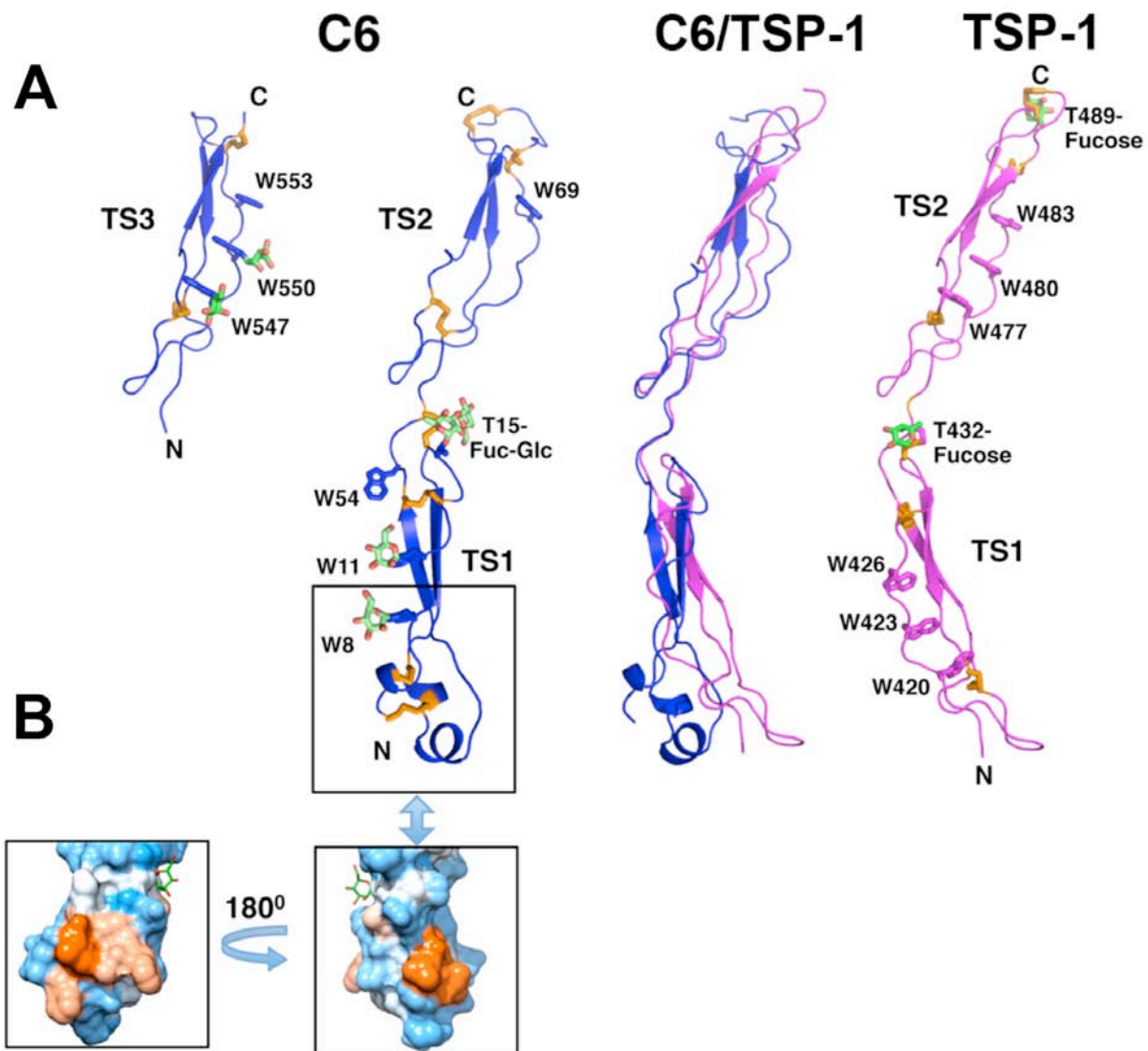
CH1
 C6 265 - -I^FY^SS^SK^RS^EN^IN^HN^SA^FK^QA^IQ^AS^HK^DS^SF^IR^IH^KV^MK^VL^NF-T^TK^AK^DL^HL^SD^VF^L 318
 C7 204 - - -F^RS^SS^SS^SR^SY^TS^HT^NE^IH^KG^SY^QL^LV^VE^NT^VE^VA^QF^IN^NN^PE^FL^QL^AE^PF^W 255
 C8 β 208 - -G^IF^EL^GI^SS^QS^DR^GK^HY^IR^RT^KR^FS^HT^KS^VF^LH^AR^SD^LE^VA^HY-K^LK^PR^SL^ML^HY^EF^L 264
 C8 α 229 - -S^PL^LV^GV^GV^SH^SQ^DT^SF^LN^EL^NK^YN^EK^KF^IF^TR^IF^TK^VQ^TA^HF-K^MR^KD^DI^ML^DE^GM^L 285
 C9 241 I^SL^HG^KG^SF^RF^SY^SK^NE^TY^QL^FL^SY^SS^KK^EK^MF^LH^VK^GE^IH^LG^RF-V^MR^NR^DV^VL^TT^TF^V 299

MACPF CH2
 C6 319 K^AL^NH^LP^LE^YN^SA^LY^SR^IF^DD^FG^TH^YF^TS^GS^LG^GV^YD^LL^YQ^FS^SE^EL^KN^SG^LT^EE^EA^KH^C 378
 C7 256 K^EL^SH^LP^SL^YD^YS^AY^RR^LI^DQ^YG^TH^YL^QS^GS^LG^GE^YR^VL^FY^VD^SE^KL^KQ^ND^FN^SV^EE^KK^C 315
 C8 β 265 Q^RV^KR^LP^LE^YS^YG^EY^RD^LF^RD^FG^TH^YI^TE^AV^LG^GI^YE^YT^LV^MN^KE^AM^ER^GD^YT^LN^NV^HA^C 324
 C8 α 286 Q^SL^ME^LP^DQ^YN^YG^MY^AK^FI^ND^YG^TH^YI^TS^GS^MG^GI^YE^YI^LV^ID^KA^KM^ES^LG^IT^SR^DI^TT^C 345
 C9 300 D^DI^KA^LP^TT^YE^KG^EY^FA^FL^ET^YG^TH^YS^SS^GS^LG^GL^YE^LI^YV^LD^KA^SM^KR^KG^VE^LK^DI^KR^C 359

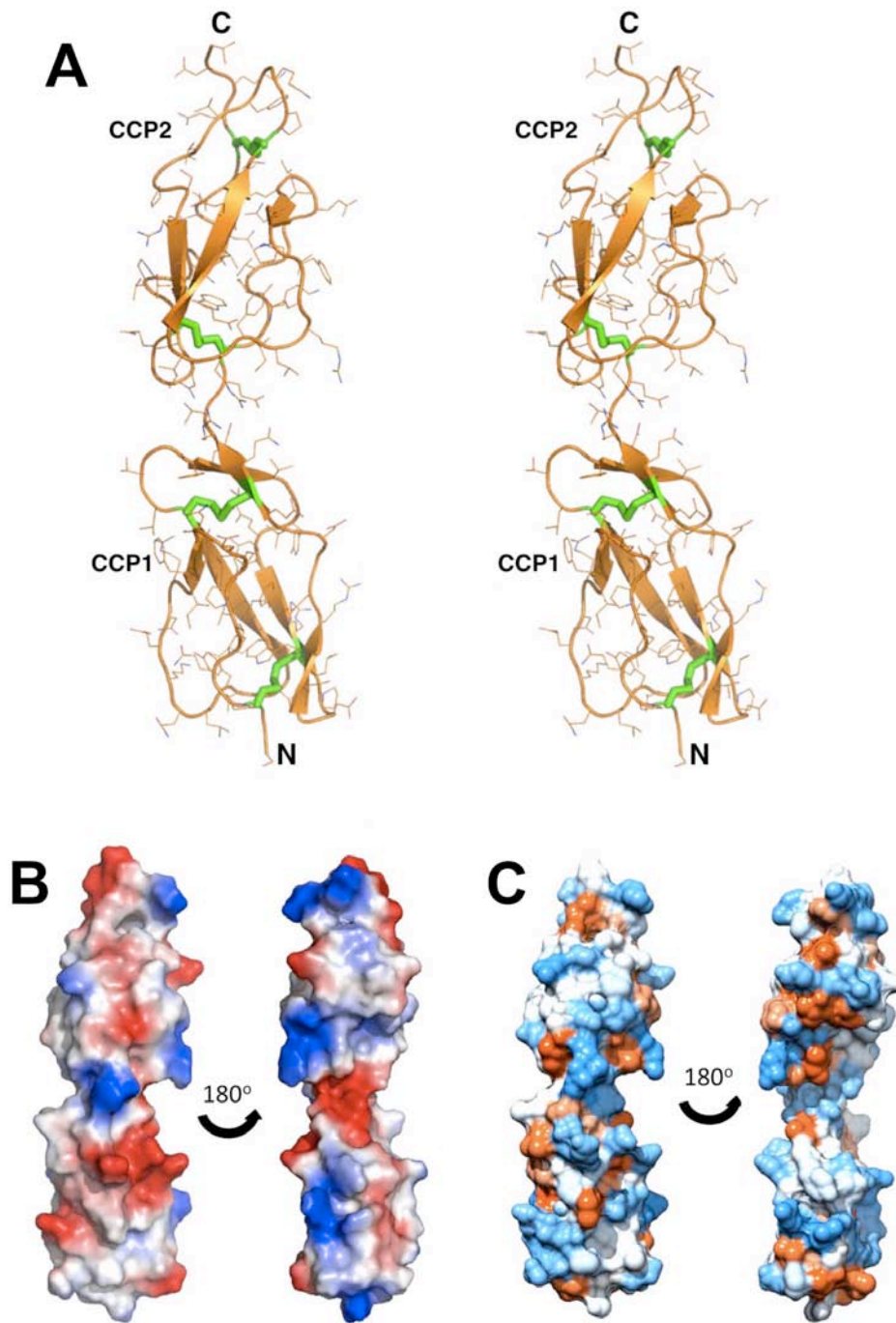
CH2 CH3
 C6 379 V^RI^ET^TK^KR^VL- - -F^AK^KT^KV^EH^RC^TT^NK^LS^EK^HE^GS^FI^QG^AE^KS^IS^LI^RG^GR^SE^YG^AA^L 434
 C7 316 K^SS^GW^HF- - -V^VK^SS^HG^CK^EL^EN^AL^KA^AS^GT^QN^NV^LR^GE^PF^IR^GG^GA^GF^IS^GL 365
 C8 β 325 A^KN^DF^KI^GG^AI^EE^VY^VS^LG^VS^VG^KC^RG^IL^NE^IK^DR^NK^RD^TM^VE^DL^VV^LV^RG^GA^SE^HI^TT^L 384
 C8 α 346 F^GG^SL^GI^QY^E-D^KI^NV^GG^LS^GD^HC^KK^FG^GG^KT^ER^AR^KA^MA^VE^DI^IS^RV^RG^GS^GW^SG^GL 404
 C9 360 L^CY^HL^DV^SL^AF^SE^IS^VG^AE^FN^KD^DC^VK^RG^EG^RA^VN^IT^SE^NL^ID^DV^VS^LI^RG^GT^RK^YA^FE^L 419



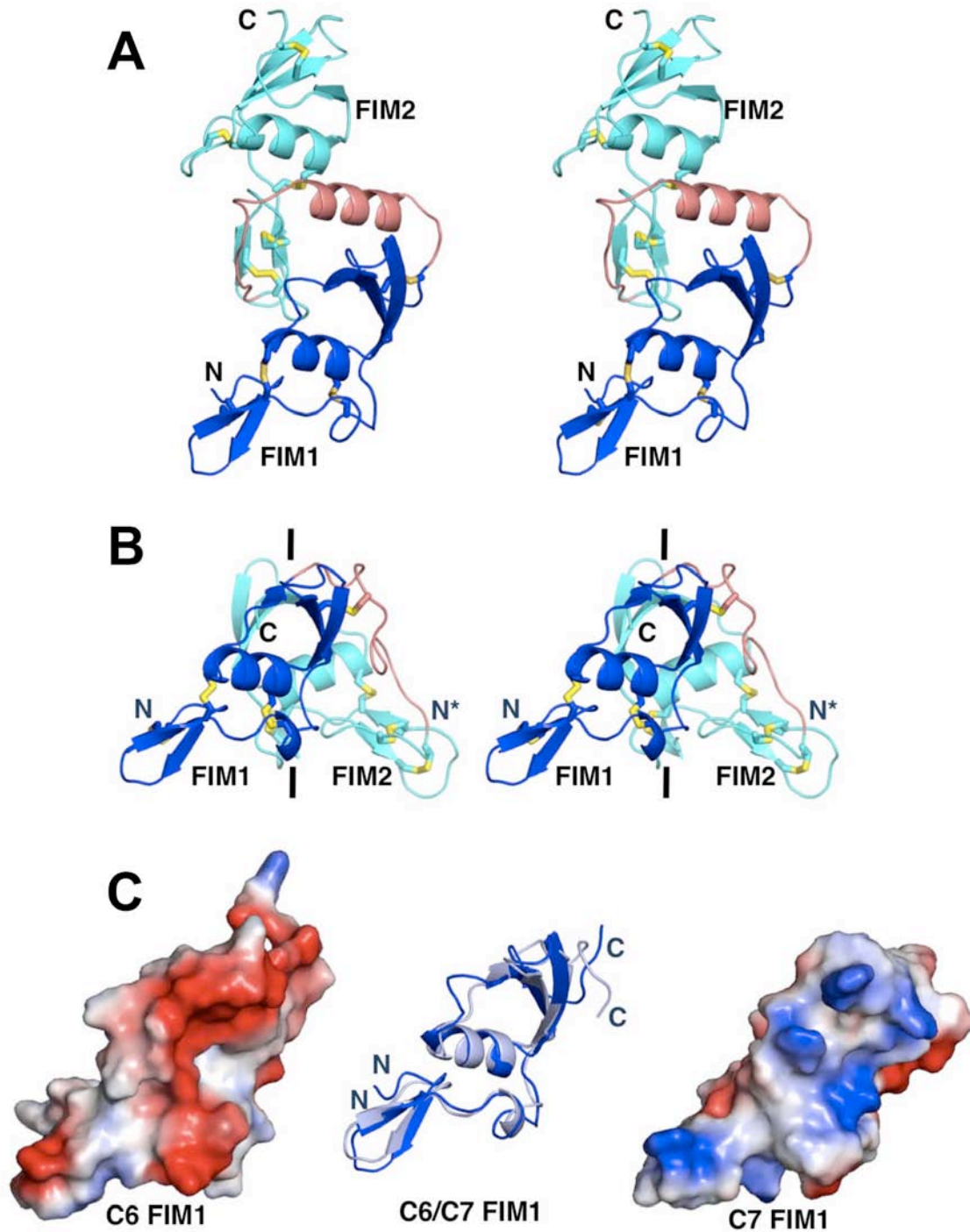
Supplemental Fig. 2. Multiple sequence alignment of MAC components C6-C9 (2 pages). Arrows (β -sheet) and cylinders (α -helix) indicate the secondary structure elements of C6. Colored bars above sequences indicate the C6 domains/modules. Aligned residues are colored according to the ClustalX scheme. In CH1 and CH2, the hydrophobic residues of the putative transmembrane hairpins are highlighted by pink backgrounds, and the regions predicted to lie on the periplasmic side are highlighted by cyan backgrounds. Ca^{2+} -coordinating residues in the LR domain are marked with asterisks.



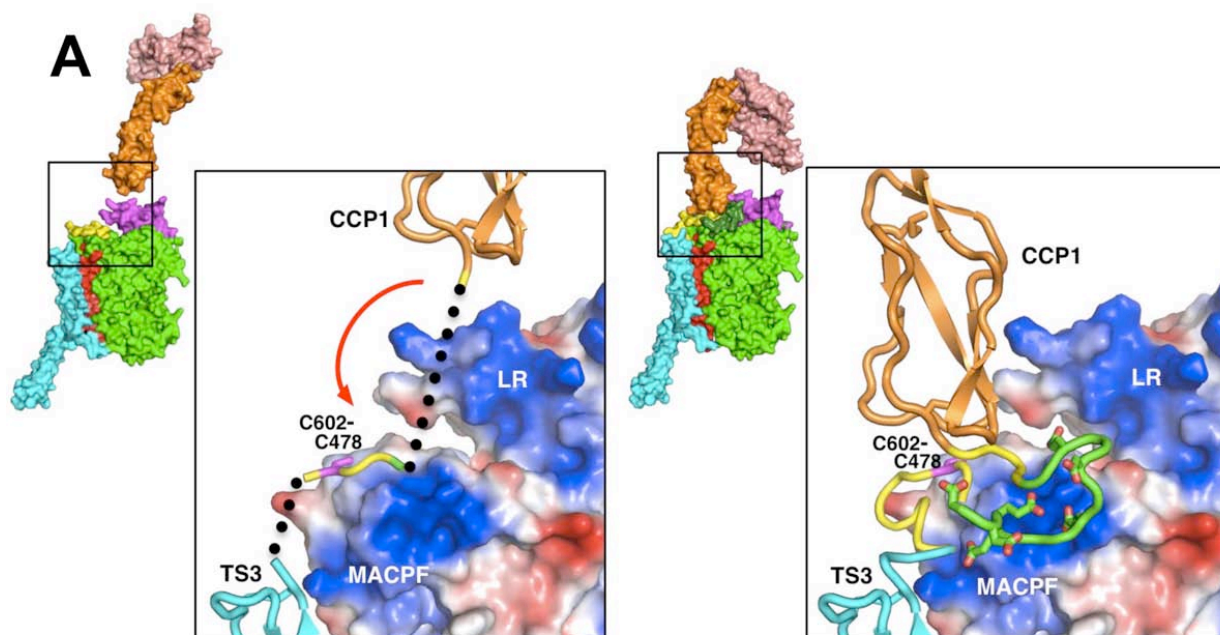
Supplemental Fig. 3. Comparison of TS modules from C6 (in blue) and thrombospondin-1 (TSP-1) (in magenta). *A*, Despite differences in crystal contacts, pairs of TS modules from C6 and thrombospondin-1 (PDB entry 1LSL) have similar rod-like conformations, presumably due to the presence of conserved prolines (Pro58 and Pro472), disulfide bonds (Cys18-Cys57 and Cys433-Cys471), and O-glycosylation (Thr15 in C6) in their linkers. TS modules are often C1-mannosylated at the first two tryptophans of a WxxWxxW motif, as seen in TS3 of C6. Although TS1 of C6 has only 2 of the 3 Trps of the canonical linear motif, it is still mannosylated at two tryptophans, presumably because Trp54 occupies the physical position of the “missing” Trp14. This would suggest that mannosylation occurs after folding into the final 3-D structure. Note that while both TS modules of thrombospondin-1 contain the canonical motif, the protein was expressed in insect cells, which lack the mannosylation pathway. Sugars are shown as green/red sticks, disulfide bonds as yellow sticks. For clarity, sugars/disulfides are not shown on the superposed C6/TSP-1 pair. *B*, TS1 of C6 has an unusual helical conformation at its tip (shown in 3 boxes). Two inserts present hydrophobic patches (lower boxes show surface models colored by hydrophobicity, increasing from blue to orange), which may participate in membrane binding.



Supplemental Fig. 4. Stereo and surface presentations of the CCP module of C6. *A*, Stereo pair of the 2 domains comprising the CCP module, shown as secondary structure cartoon with side-chains (thin sticks) and disulfide bonds (thick green sticks). *B*, Solvent accessible surface colored according to electrostatic potential (positive is blue, negative is red). First view is same as in *A*; second is rotated by 180° about a vertical axis. Note the opposite/complementary charges. *C*, Surface hydrophobicity (increasing from blue to orange). Views are the same as in *B*.



Supplemental Fig. 5. Ribbon and surface presentations of FIM modules from C6 and C7. *A* and *B*, Stereo views of FIM modules from *A*, C6 and *B*, C7 (PDB entry 2WCY). FIM1 is blue, the linker is brown, and FIM2 is cyan. All views have FIM1 in the same orientation. The dimer of C7 FIMs has 2-fold pseudo-symmetry (axis indicated by black bars). *C*, Superposition of FIM1 from C6 and C7 (at center) illustrates close structural homology (RMS deviation is 1.0 Å for 40 of 60 C α atoms). Nevertheless, their putative C5b-binding faces (shown as electrostatic surface potentials (red/blue are negative/positive)) have distinct shapes and opposite charges.



B

	TS3	L1 *		L2		*	L3	CCP1		
C6 human 587	EED	CTFS	IENNGQP	CIN	DD	EMKEVDLP	EIE	-----	ADSGCPQP	626
C6 bovine 587	EEH	CTFS	IMQNDGQP	CIS	DD	EMKETDLP	ELE	-----	SDSGCPQP	626
C6 mouse 587	EED	CTVS	IMENVGQP	CIN	DD	EMTEVDLA	EPE	-----	AESGCSQP	626
C6 frog 591	EED	CSIS	LFEDTGAL	CIN	DE	DKKEVDQE	EPE	-----	RDSGCPKP	630
C7 human 520	STQC	-----	-----	-----	DE	ELEHLRLL	EPC	FPLSLVPT	EFCPS	552
C7 bovine 520	TRQC	-----	-----	-----	ED	ELEHLRLL	EPC	FPLSLVPT	EFCSS	552
C7 mouse 520	SKQC	-----	-----	-----	ED	QLEKLRLL	EPC	FHSSLAPK	EFCSS	552
C7 frog 510	SEL	-----	-----	-----	ED	SELEHLRTV	EPC	FDISIVPT	EFCPP	542

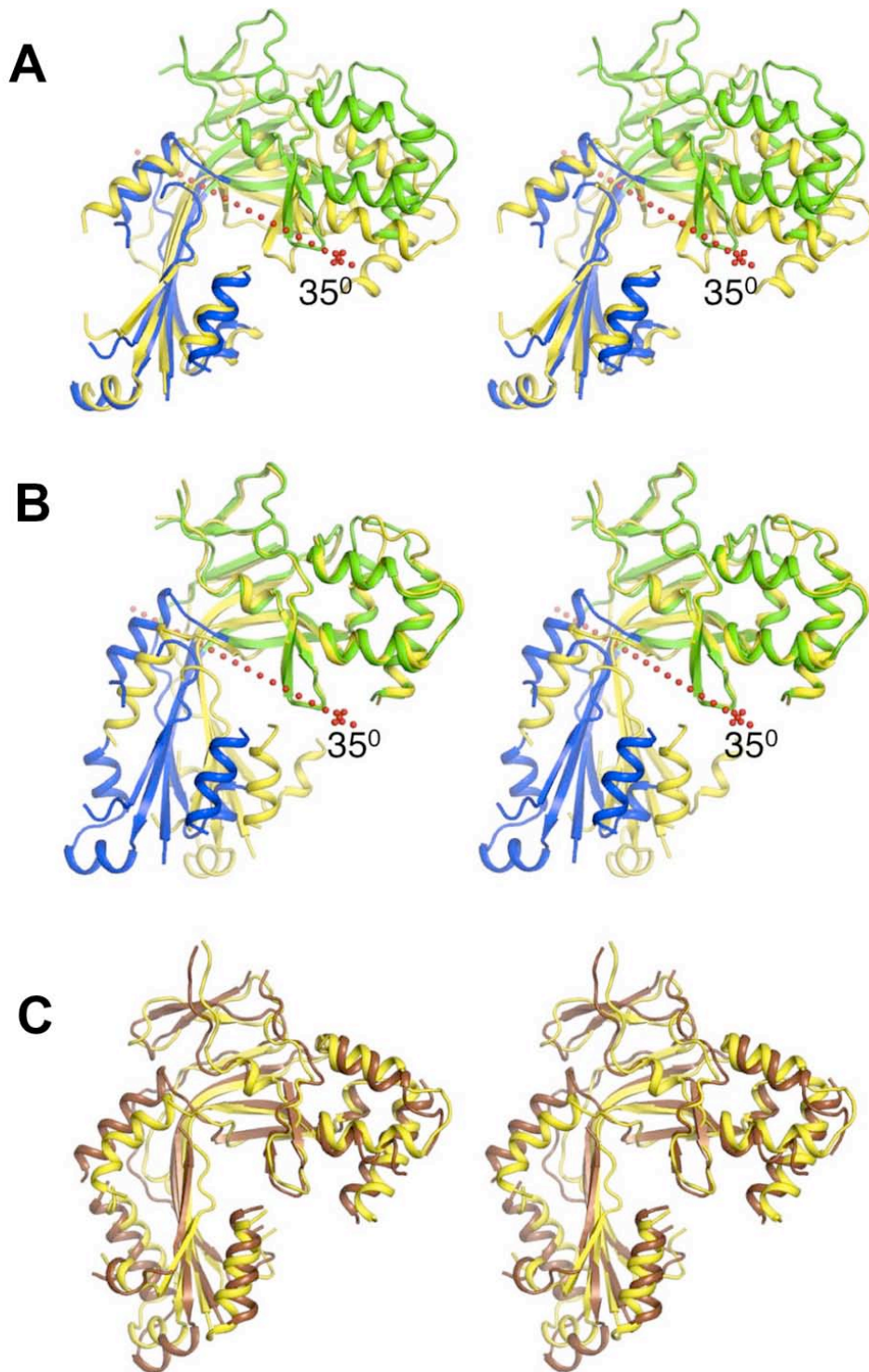
Conservation

Hydrophobic

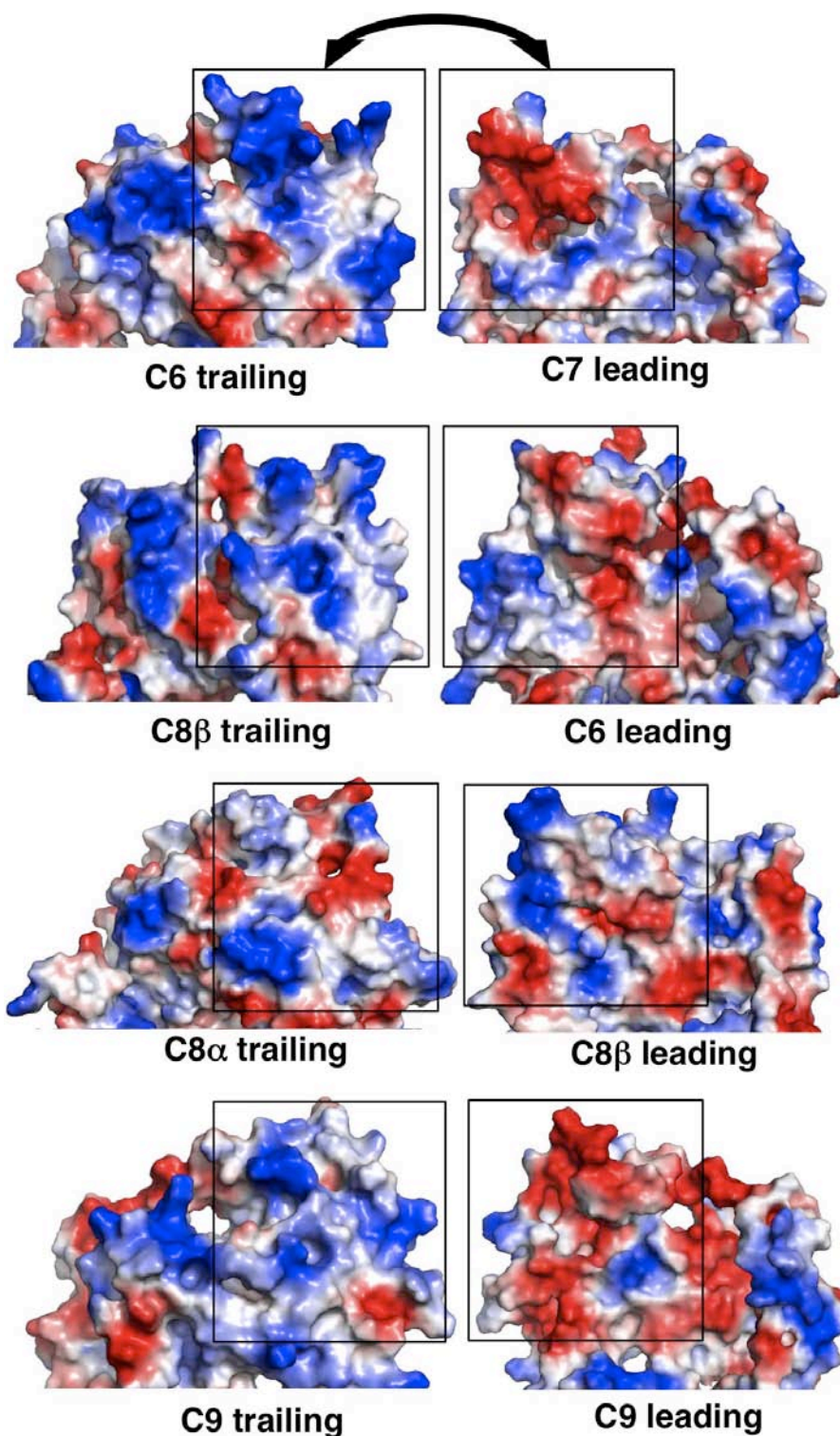
Aliphatic

Charged

Supplemental Fig. 6. Modeling the position of CCP/FIMs in native C6. *A*, On the left, CCP/FIMs are dissociated from each other and from MACPF as seen in the crystal structure of C6; on the right, CCP/FIMs and the TS3-CCP linker are modeled to attach to MACPF near a conserved disulfide bond, Cys478-Cys602. This position of CCP/FIMs corresponds to the electron microscopic images of C6 and C7. *B*, Sequence comparison of the TS3-CCP1 linkers in C6 and C7 from different vertebrates. The colors from pink to blue indicate hydrophobicity/charge, and their intensity indicates amino acid conservation (prepared with ClustalW). The yellow fragments of linkers (L1 and L3) in both C6 and C7 make a disulfide bond to MACPF, but the conserved cysteines (marked with a star) have different positions with respect to a conserved negatively charged fragment L2. This rearrangement of the linker fragments suggests that in native C6 and C7, their linkers should have compact folds that interact with similar fragments of MACPF. We propose that the negatively charged fragment L2 binds to the positively charged area of MACPF. In the C5b-C6 complex, L2 may bind to the positively charged surfaces of LR or C5b.



Supplemental Fig. 7. Stereo views of superposed MACPFs in different reference frames and overlay with perforin. *A* and *B*, MACPFs from C6 (yellow) and C8 α (green/blue) (pdb entry 3OJY) are superposed via either the upper or lower segments of MACPF. The red dotted line illustrates the apparent rotation axis. Rigid body motions were identified using the program DynDom (see Experimental Procedures). *C*, MACPFs from C6 (yellow) and perforin (brown) are superposed, showing close alignment of their β -sheets and flanking elements.



Supplemental Fig. 8. Complementary charges on putative interacting surfaces of MAC components. The black boxes indicate structurally conserved areas in MACPF and LR (the sides of the “Wedge”) that form the real (C8 α -C8 β) or putative interfaces in the mature MAC (surfaces colored according to charges - red/blue = negative/positive). Note the complementary charges in each case. C7 and C9 were modeled by threading their sequences on the C6 structure.

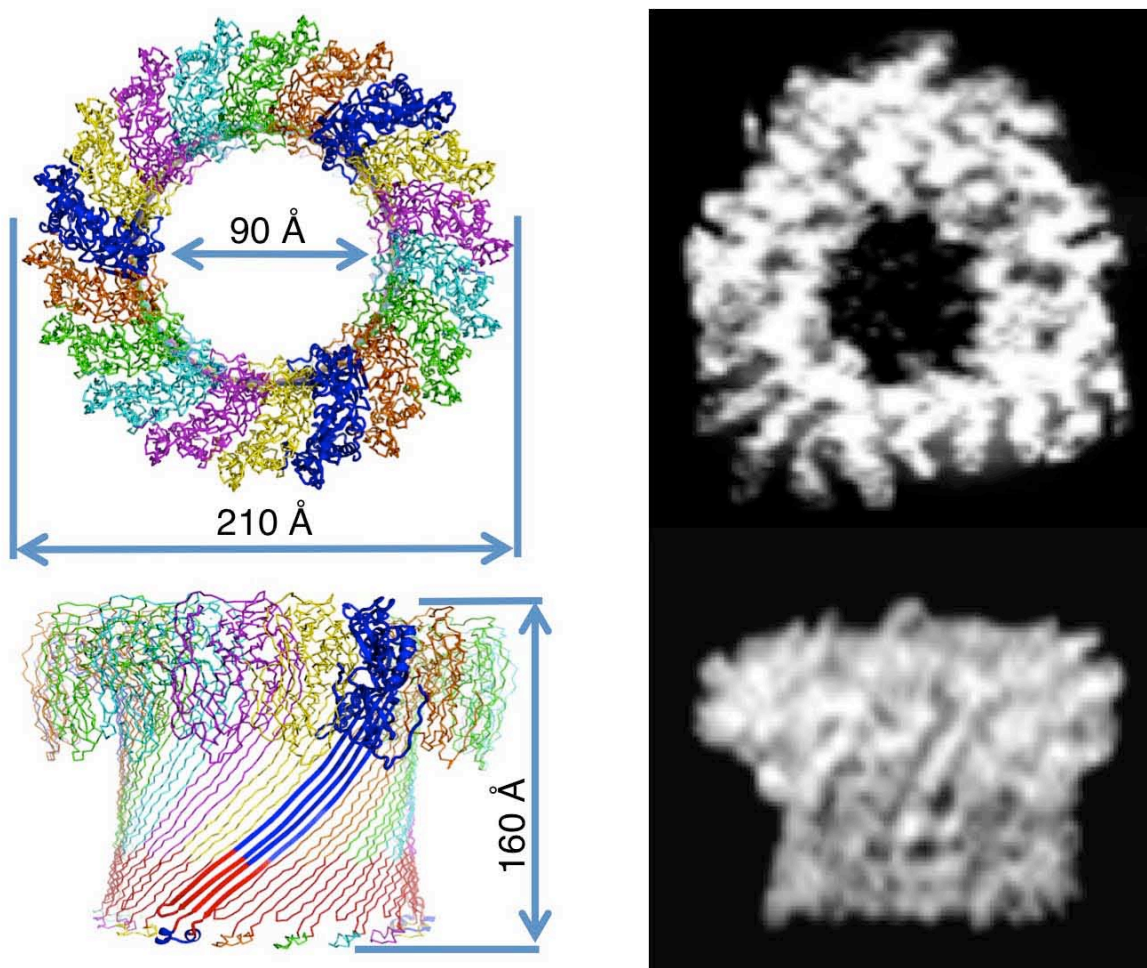
C6 Human	F	Y	K	D	L	T	S	L	G	H	N	E	N	Q	Q	G	S	F	S	S	Q	G	G	S	S	F	S	V	P	I	F	Y	S	S	K	R	S	E	N	I	N	H	N	S	A	F	K	Q	A	I	Q	A	S	H	K	K	D	S	S
C6 Bovine	F	Y	D	D	L	I	P	L	E	D	N	K	D	Q	E	A	L	G	S	G	L	A	T	S	S	F	R	V	P	I	F	Y	S	S	K	R	S	Q	S	S	H	S	S	A	F	K	Q	A	I	Q	A	S	Q	K	K	A	S	S	
C6 Mice	F	Y	K	N	L	I	S	F	E	K	N	K	N	E	D	S	L	S	V	D	E	R	T	K	F	F	P	I	P	I	F	H	F	S	E	K	N	E	H	S	H	S	S	A	F	N	K	V	I	K	A	S	H	K	K	D	S	S	
C6 Xenopus	L	H	K	S	L	I	P	F	S	D	E	N	K	R	H	G	L	S	V	G	R	W	S	G	S	G	I	P	W	L	W	H	T	G	T	S	T	K	S	W	A	S	S	S	F	R	E	A	I	T	A	T	R	Q	K	S	S	K	
C7 Human	F	Y	N	S	T	W	S	Y	V	K	H	T	S	T	E	H	S	S	S	R	K	R	---	S	F	F	R	---	S	S	S	S	S	S	S	R	S	Y	T	S	H	T	N	E	I	---	H	K	G	K	S	Y	Q						
C7 Bovine	F	Y	N	S	T	W	A	Y	V	K	E	T	S	T	E	H	S	S	S	K	G	R	---	F	L	F	F	---	S	S	S	S	S	H	G	Y	S	S	N	T	N	I	L	---	T	K	K	K	S	Y	Q								
C7 Mouse	F	Y	N	S	S	W	S	Y	I	K	H	T	S	T	E	Q	N	T	F	Y	S	W	K	---	G	L	F	---	S	H	S	R	N	T	Y	G	H	G	S	A	K	E	E	I	D	T	K	M	K	S	Y	Q							
C7 Xenopus	F	Y	S	S	W	S	Y	V	K	E	T	E	S	R	---	E	---	---	---	---	---	---	---	---	---	---	---	---	---	---	T	T	S	N	H	G	Y	Y	H	Y	H	K	D	T	Q	S	N	T	K	E	K	N	Y	Q					

CH1

C6 Human	Q	F	S	S	E	E	L	K	N	S	G	L	T	E	E	A	K	H	C	V	R	I	E	T	K	---	K	R	V	L	F	A	K	K	T	K	V	E	H	R	C	T	N	K	L	S	E	K	H	E	G	S	F	I	Q	G	A	E
C6 Bovine	Q	F	S	K	E	L	K	N	S	G	L	T	Q	E	E	A	K	N	C	I	R	I	E	T	K	---	K	R	F	L	F	V	K	K	T	K	V	E	H	R	C	T	N	K	L	S	E	K	Y	E	G	S	F	M	Q	G	S	E
C6 Mice	Q	F	S	R	Q	E	L	Q	N	S	G	L	T	E	E	A	Q	N	C	V	Q	Y	E	T	K	---	K	L	F	L	Y	M	---	E	I	H	K	E	D	T	C	T	N	K	L	S	E	K	Y	G	G	S	F	L	Q	G	S	E
C6 Xenopus	Q	Y	S	T	E	N	V	Q	S	S	G	L	T	D	Q	E	M	A	H	C	V	F	E	E	I	R	T	R	R	F	F	F	V	K	T	H	R	T	C	T	N	K	M	T	E	R	Y	S	G	S	F	L	Q	S	S	E		
C7 Human	Y	V	D	S	E	K	L	K	Q	N	D	F	N	S	V	E	E	K	K	C	K	S	---	S	G	W	H	F	V	V	K	F	S	S	---	H	G	C	K	E	L	E	N	A	L	K	A	A	S	G	T	Q	N	N	V	L		
C7 Bovine	H	M	D	S	E	K	V	K	K	F	D	F	H	S	E	D	K	R	K	C	A	S	---	S	H	F	Q	F	L	F	T	S	S	K	---	Q	K	C	T	M	E	E	V	L	K	S	V	E	N	E	G	N	L	L				
C7 Mouse	Y	V	D	S	G	S	A	K	E	T	G	F	Q	S	D	Q	D	N	A	C	S	S	---	A	D	F	Q	F	L	F	T	S	S	A	D	---	Q	R	C	M	K	Q	L	E	T	E	K	S	T	S	G	N	K	G	R	L		
C7 Xenopus	Y	L	D	S	E	K	I	T	A	N	G	V	T	K	R	D	M	Q	S	C	T	S	---	S	S	K	N	F	F	F	V	K	Y	S	S	---	K	E	C	K	A	L	N	E	V	I	R	Q	S	S	G	S	T	D	R	E	V	

CH2

Supplemental Fig. 9. Sequence alignment of CH1 and CH2 (putative membrane-inserting elements) from vertebrate orthologs of C6 and C7. The red boxes indicate hydrophobic patches at the predicted tips of β -hairpins that may attach the C5b-7 complex to the membrane. The CH2 hairpins of most C7s are 5 residues shorter than in C6. Note, however, that CH1 of Xenopus C7 is 20 residues shorter than its C6, and thus appears to lack a membrane-binding hairpin altogether. The shorter C7 is consistent with a model in which C7 is located at the trailing edge where growth of the immature MAC pore does not occur. The background colors correspond to the ClustalX scheme.



Supplemental Fig. 10. Atomic model of the poly-C9 pore containing 18 subunits The atomic model (at left) is compared with EM images of poly-C9 (at right). The protrusions evident in the upper micrograph may be TS2 domains. Note the tilt of the β -hairpins evident in the barrel (lower micrograph)